

We are IntechOpen, the world's leading publisher of Open Access books Built by scientists, for scientists

4,800

Open access books available

122,000

International authors and editors

135M

Downloads

Our authors are among the

154

Countries delivered to

TOP 1%

most cited scientists

12.2%

Contributors from top 500 universities



WEB OF SCIENCE™

Selection of our books indexed in the Book Citation Index
in Web of Science™ Core Collection (BKCI)

Interested in publishing with us?
Contact book.department@intechopen.com

Numbers displayed above are based on latest data collected.

For more information visit www.intechopen.com



Lightning Energy: A Lab Scale System

Mohd Farriz Basar, Musa Yusop Lada and Norhaslinda Hasim
*Universiti Teknikal Malaysia Melaka (UTeM),
Malaysia*

1. Introduction

This chapter which has six subchapters explains the energy storage system in harvesting a lightning return stroke for a lab scale system. Nowadays, the world is facing the energy crisis and consequently a renewable energy is required as an energy contributor to solve the crisis. Hence, it is believed that lightning return stroke has a good future to be a free electricity sources. The main difficulty in harnessing the lightning stroke is to attract and simultaneously to store the energy, which limited in a microsecond. Due to that, the computer simulation works using PSpice is done as the preliminary effort intended for the hardware development as well as to understand and verify the proposed system. A lab scale system is set up based on natural characteristics of lightning to determine the performance of the sample capacitor as energy storage accurately. Hence, the single stroke impulse voltage is used as a mock of lightning. Regarding the energy storage device, the capacitor is employed due to the reliability, cost-effective and it is the most common. In addition, the direct tapping system and the high speed switching is most wanted in order to make the whole system more realistic. The capacitors are subjected to 1.2/50 μ s, 4,200V single-stroke impulse voltages generated by a single stage impulse generator. In this chapter, the energy of impulse voltage that successfully transferred and stored in the storage capacitors is discussed. Basically, the efficiency of the energy transfer is depends on the capacitance values and the switching times. As a final point, the lab scale system explained in this chapter demonstrates the capability to capture the energy from lightning return strokes that can be a clean energy sources.

On the other side, lightning which have extremely high current and high voltage is a gratis electricity energy sources that can be replenished. The lab scales systems for harvesting the energy from lightning return stroke, which discussed in this chapter able to give a new contribution to solve the energy crisis and it will be very challenging. Up until now, the mature technology in harvesting the lightning stroke for the large-scale system is still not yet ready and the relevant scientific literature is not easily found. It noted that the final system proposed in this chapter would provide an understanding of the system principle and additionally provide a noteworthy contribution for further research.

2. Clouds and lightning

Lightning return stroke is a complex phenomenon. The large peak currents or the electromagnetic shock wave are capable to kill people and destroy the buildings, trees, animals as well as electrical appliances. As a result, the damage can be outstanding in term of cost.

2.1 Clouds

Most researches on the electrical structure of clouds have focused on the cumulonimbus, the familiar thundercloud or thunderstorm, because this cloud type produces most of the lightning. There have been limited studies of the electrical properties of other types of clouds such as stratus, stratocumulus, cumulus, nimbostratus and cirrus clouds [2].

Briefly, clouds carry positive and negative charges. Through the dynamic of nature, clouds distribute these charges and collect negative charges at its bottom as well as positive charges at the top. After going through all the processes, charge at the bottom of the cloud draws and equal in magnitude but opposite polarity charge at the ground level. This creates a look like capacitor system between the cloud and the ground where the dielectric is air [3]. During stormy weather, the dynamic mechanism of the cloud will increase the charge density at clouds until threshold is reached and air loses its dielectric. Subsequently, lightning discharge occurs where air becomes conductor and simultaneously the charge travel from cloud to ground.

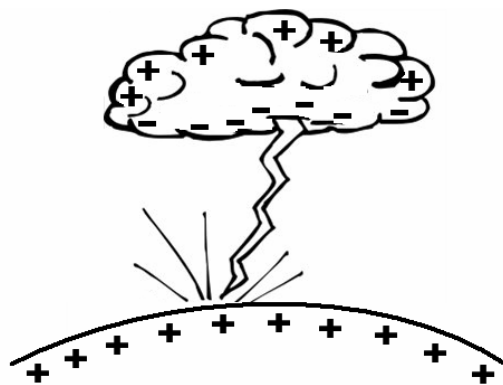


Fig. 1. Thundercloud charge distribution of lightning between cloud and ground

Thundercloud charge distribution of lightning between cloud and earth have been identified which is shown in Figure 1. There are different types of lightning like example the upward-initiated flashes; are relatively rare and usually occur from mountain peaks and tall man-made structures. Cloud-to-ground lightning has been studied more comprehensively than other form of lightning because of it is happen regularly surrounding us. It is known that lightning strike involves very large and very fast impulse voltage and current. It is flow to the ground, which in turn produces the corresponding electromagnetic fields.

Previous studies on lightning as an electrical energy and the possibilities of harnessing the lightning energy have been since 1752 starting with Benjamin Franklin observation on characteristics of lightning behavior. The estimation the lightning strike to the surface of earth is 100 time every one second. The challenge with lightning is to suggest a storage device to distribute the lightning power that it can be extracted later and the critical aspect on safety capture need to be alert. Data from NASA's lightning imaging sensor shows that the lightning occurs frequently over the land compare to the water. About 90% of lightning phenomenon happens in the land in spite of 75% of earth cover by the water.

2.2 Mock lightning

In this lab scale system, it proposed to use single impulse voltage $1.2/50\mu\text{s}$ as a mock lightning. It can be obtained by using the single stage impulse voltage generator. An

impulse voltage is a unidirectional voltage which characterized by two time intervals expressed in microseconds, μs which is wave front time, t_f and wave tail time, t_t . Figure 2 shows the impulse voltage waveform that rises rapidly to a maximum value and then decays slowly to zero.

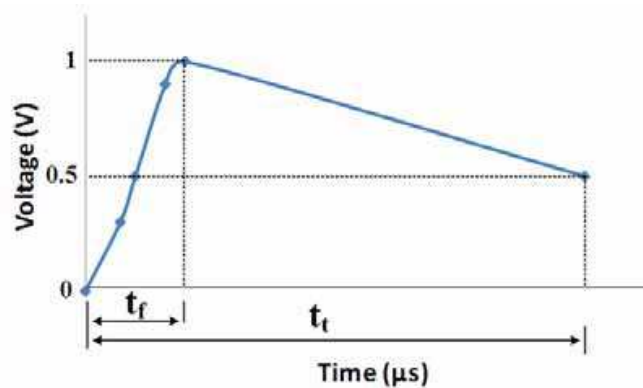


Fig. 2. Standardized impulse voltage wave shape

According to the standard wave shapes, the time to peak value or front time, t_f is set to be $1.2\mu\text{s}$ with the tolerances is $\pm 30\%$. Thus, the system proposed must capable to attract and stored the voltage at this peak time. Besides that, the tail time, t_t is set to be $50\mu\text{s}$ with the tolerances is $\pm 20\%$. The time to half value of the wave tail of an impulse voltage is the total time occupied by the impulse voltage in rising to peak value and declining there form to half the peak value of the impulse.

3. Energy storage

Energy storage technologies do not represent energy sources, but they provide valuable added benefits to improve power quality, stability and reliability of supply. In this modern power application, practicable storage technologies also known as viable storage technologies like batteries, flywheels, ultra capacitors and superconducting energy storage system was rapidly used. Figure 3 shows a specific energy ranges versus specific power.

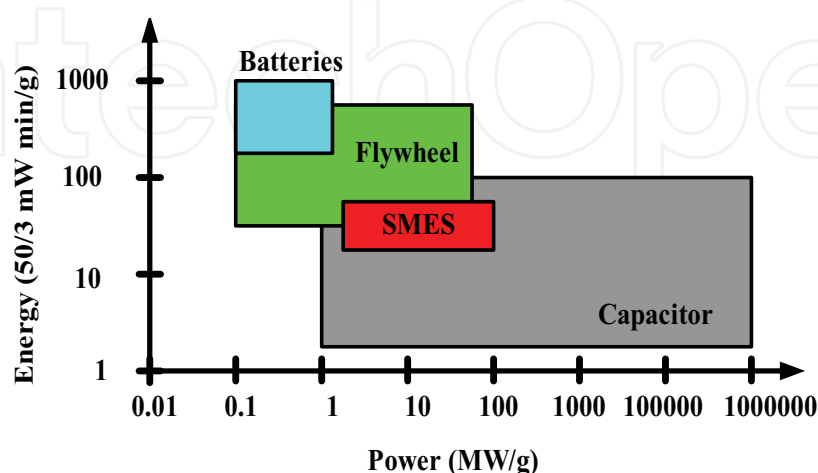


Fig. 3. Specific power versus specific energy ranges

Optimal Energy System (OES) that consist of flywheel based energy storage system currently be manufacture and design to provide pulse of energy for charging high voltage capacitor. This system has been used for electromagnetic air-craft launch system (EMALS) applications. Flywheel technology has been considered an attractive energy storage choice due to its potential for reduced weight and volume, high duty-cycle tolerance, and low maintenance requirements. Flywheel technology overcomes some of the shortcomings of today's energy storage systems by having an extremely high cyclic-life, limited temperature sensitivity, no chemical hazards, charge rate equal to discharge, and reduced weight and space.

They are a few benefits of adding energy storage to power electronic compensators for utility application such as improved system reliability, dynamic stability, enhanced power quality, transmission capacity enhancement and area protection. It shows that energy storage devices can be integrated to power electronics converters to provide power system stability, enhanced transmission capability, and improved power quality. Adding energy storage to power electronics compensators not only enhances the performances of the device, but can also provide the possibility of reducing the MVA ratings requirements of the front-end power electronics conversion system. This is an important benefit consideration when considering adding energy storage systems.

Supercapacitor was an advanced technology as compared to battery or electrostatic capacitor. The advantage of supercapacitor is high fast step response in term of charge and discharging. Effects of supercapacitor on power system application are absorbing high frequency power surges, reduce the degree of discharge and reduce the power losses.

In order to look into the capability of the lab scale system proposed for harvesting the lightning energy, two different types of sample capacitor are used. The first type is KNU 1910 Metallized Polypropylene Film Capacitors. The second type is CBB20 Axial-type Metallized Popypropylene Film Capacitor. These two types of sample capacitor used same dielectric, which is polypropylene film. The polypropylene capacitor was selected to be used in the testing because it is cheap, high temperature stability, readily available and it is widely used in high frequency, DC and pulse circuit's applications.

Many polypropylene film capacitors have a tolerance about 5% to 10%, which is adequate for many applications. In addition, there is very little change in capacitance when these capacitors are used in applications within frequency range of 100,000Hz. Moreover, the electrodes are vacuum evaporated metal on dielectric. So, the possibility for bad contact during the operation of capacitors is excluded. It also has a long life due to self-healing effect and suitable for high current.

4. High speed switching

As discussed in subchapter 2.2, the maximum value of the impulse voltage is occurred at $1.2\mu\text{s}$. Consequently, the system proposed must able to draw out and store the energy of the impulse voltage (mock lightning) particularly at that extremely short time. Hence, the high speed switching is imperative to isolate the sample capacitor from any connection once the energy enters the sample capacitor. As a result, the potential voltage that can be retained or sustained in the sample capacitor can be investigate.

Figure 4 shows the block diagram of the high speed switching circuit that is used in the experimental work. The high speed switching controller consists of a microcontroller, a gate drive and a switching device and the orientation of components is shown in Figure 5.

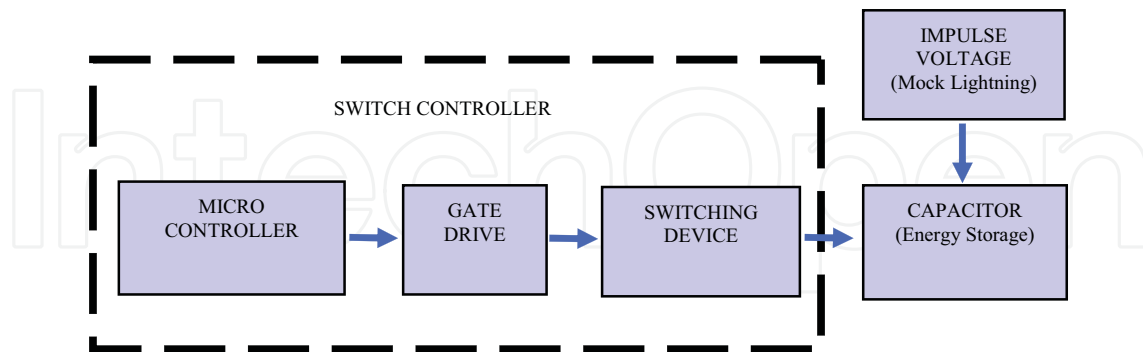


Fig. 4. Block diagram of the high speed switching circuit

4.1 High speed switching components

The advantages of this switching circuit are the circuit is simple and the cost is low. The main components that are used in the circuit are indicated in the Table 1. The high voltage IGBT is preferred to use as a switching device because it has a tremendous performance and widely used. The type of IGBT that be used are NPT (Non Punch Through) type, which is low efficient emitter and high carrier lifetime compare to others types of IGBT.

	Components	Description
Micro Controller	PIC 16F84A	<ul style="list-style-type: none"> • It is a peripheral interface controller • 16 series PIC, 14 bit (instructions) microcontroller • Maximum operating frequency is 20MHz
Gate Drive	NPN Transistor	<ul style="list-style-type: none"> • Part Number : BC548B • Manufacturer : Fairchild Semiconductor
Switching Device	High Voltage IGBT	<ul style="list-style-type: none"> • Part Number : IXGR 16N170AH1 • Manufacturer : IXYS

Table 1. Main components of switching controller

The micro controller circuit and gate drive requires 5Vdc of supply whilst the high voltage IGBT (switching device) requires 15Vdc to turn ON and 0Vdc to turn OFF as illustrated in Figure 6. Meanwhile, in Figure 7, to activate the switching circuit, two different level of voltage supply is required. The micro controller circuit and the gate drive requires 5Vdc of supply whilst the high voltage IGBT (switching device) requires 12Vdc.

It can see that there has an 4,200V impulse voltage at the right side of the circuit in Figure 7. At the beginning, the IGBT switch is in close position. Ideally, when the charges from the impulse voltage go into the capacitor, the IGBT switch will be open in order to isolate the capacitor to discharge. With the aid of IGBT switch, now the capacitor is like a battery.

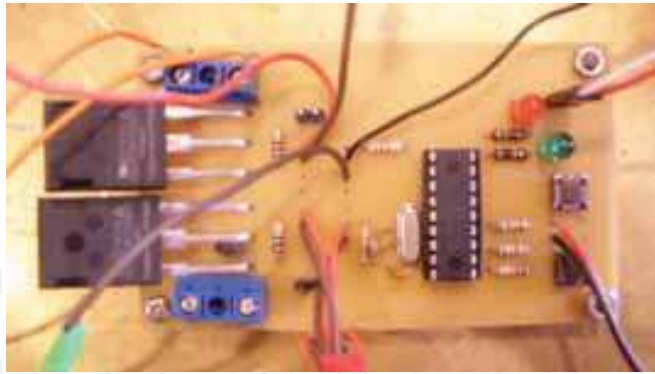


Fig. 5. Orientation of components of high speed switching controller

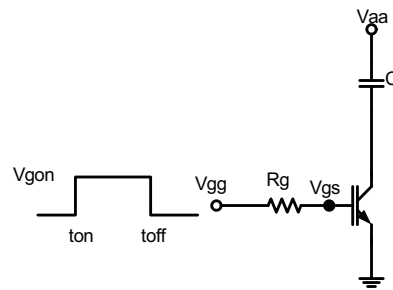


Fig. 6. Circuit diagram of IGBT with signal turn ON and OFF

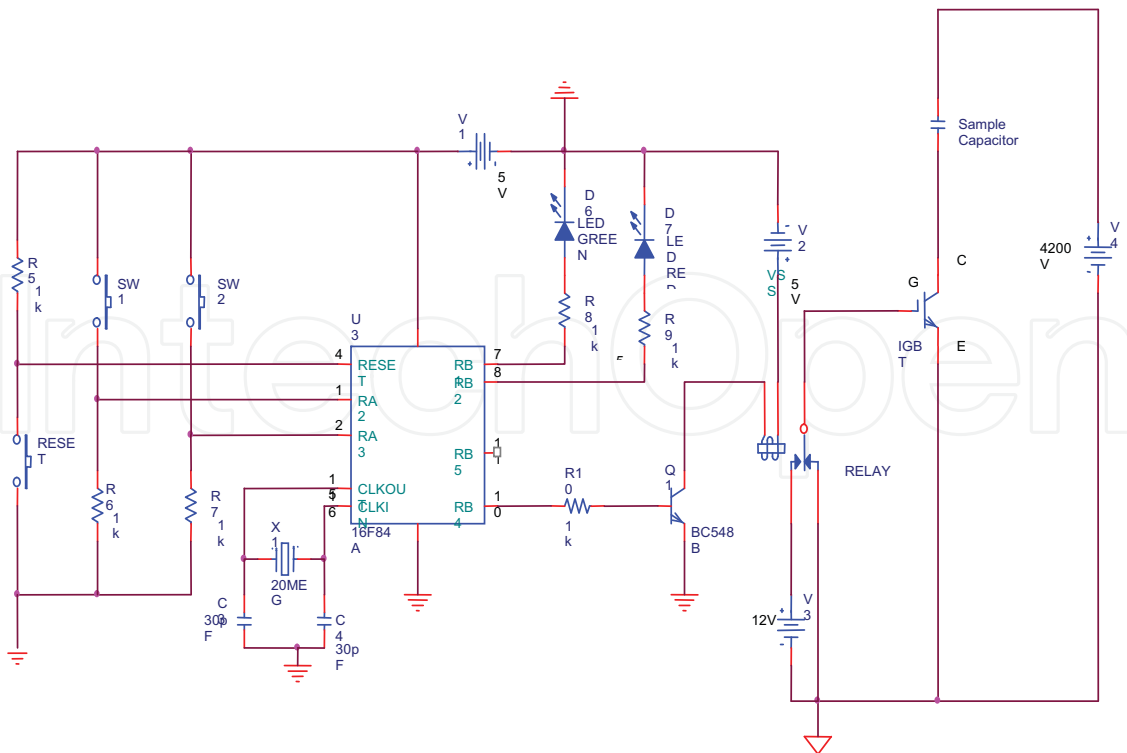


Fig. 7. Schematic diagram of the high speed switching circuit

4.2 Peripheral interface controller (PIC16F84A)

PIC is an abbreviation for Peripheral Interface Controller. It is not PLC or Programmable Logic Controller as most misunderstood, because it is an integrated chip (IC) based controller. When IC based controller is concerned, the logic levels, 0 and 1 are 0 volt and 5 volt respectively.

PIC is one of the micro technology generation and even more popular in industrial and hobbyists causing by the advantage on using it. Some of the advantage of PIC is low cost, widely available, large user base, extensive application, and serial programming capability which is the programming data of HEX (PIC data) can be write and re-write this is because PIC is made from flash memory.

A microcontroller is normally used for simple applications such as washing machines, rice cooker, air conditioner, keyboards, mouse, Liquid Crystal Displays (LCD) and much more. This means that the microcontroller is used for small applications and sometimes for standalone systems.

PIC is a brand of microcontroller, from its manufacturer, Microchip. The decision to use the PIC in this project is due to the vast employ of this device in many applications. It has Reduced Instruction Set Computer (RISC) architecture and moreover the assembly program is much simpler rather than other brands, such as Freescale (Motorola), Intel and many others. However, for the lab scale system proposed in this chapter used PIC16F84A as shown in Figure 8. Table 2 shows the function for every pin of PIC16F84A.

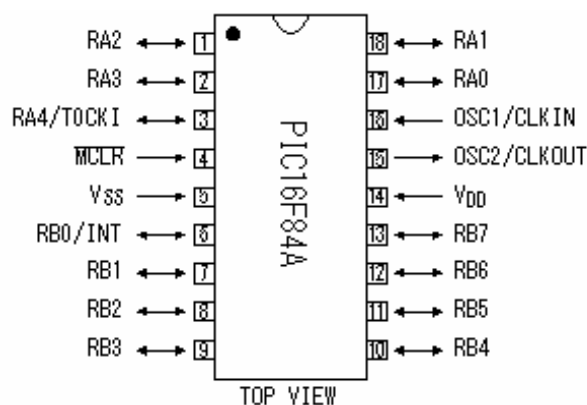


Fig. 8. Pin diagram for PIC16F84A

For programming, C language is used to write the program. Then compiler software is required to convert the C language to machine language (in zeros and ones). The compilers that have been used is mikroC. Next when the machine languages are generated, a downloader is required. The functions of this software is to transfer the machine codes of the program along with the settings to the PIC 16F84A. In simple words, the software installs the PIC with the machine codes of the program. In this project, WINPIC800 software is used because one of its advantages is that it can detect the type of PIC inserted automatically.

5. Computer simulation works

This section discuss about the computer simulation works using Pspice software. The purpose of the simulation is to obtain the testing circuit configuration that needs to be used in the experimental work. Moreover, the results of the computer simulation will verify the effort to harvest the lightning impulse voltage.

5.1 Single stage impulse voltage

The front time and the tail time of the impulse wave shape are dependently controlled by varying the value of R_D and R_E separately. The circuit arrangement for single stage impulse voltage generator involves the arrangement of high voltage dc supply from the rectifier, couple of sphere, one unit of wave shaping resistance which are wave front resistor, R_D and wave tail resistor, R_E , one unit charging capacitor C_S and one unit capacitor C_B as load capacitance. In order to obtain the single voltage impulse of 1.2/50 μ s, the value of resistance R_D and R_E can be verified by the equation 1 and equation 2.

$$t_f = 3R_D \frac{C_S C_B}{C_S + C_B} \quad (1)$$

$$t_t = 0.7(R_D + R_E)(C_S + C_B) \quad (2)$$

A capacitor C_S , previously charged to a particular dc voltage via a HV diode. It is suddenly discharged into the wave shaping network (through combination of R_D and R_E) after the breakdown or ignition of sphere gap. The sphere gap is acting as closing switch, where it is triggered by the voltage injected from the capacitor C_S .

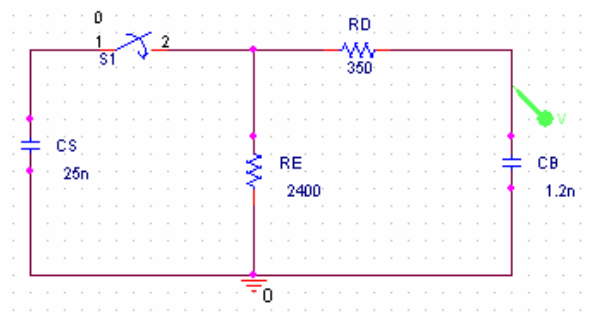


Fig. 9. Single stage impulse voltage generator simulation circuit

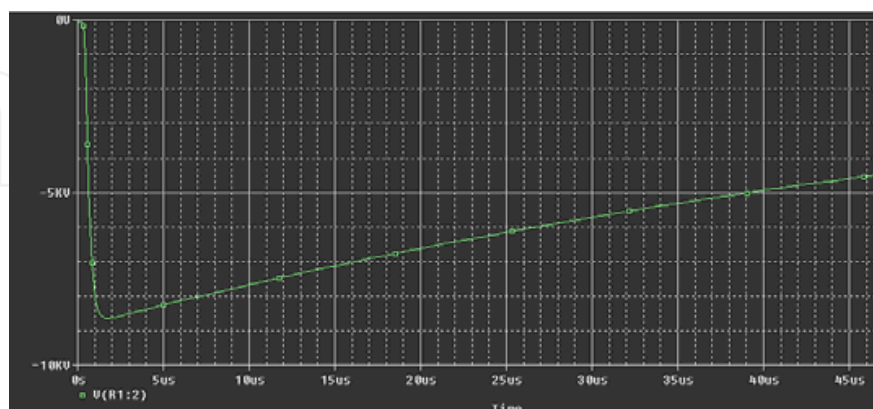


Fig. 10. Impulse voltage waveform 1.2/50 μ s

Afterward, the discharge voltage gives the desired voltage impulse wave shape. The front time and tail time can be controlled by changing the value of R_D and R_E . Switch S_1 is actually

a sphere gap. The rapid rise and slow decay impulse voltage wave shape can be generated by the activities of charging and discharging circuits with two energy storage elements, which are C_S and C_B . The C_B will be the capacitance of insulation to be tested or known as a load. As shown in Figure 9, it can see that $C_S \gg C_B$ and $R_D \gg R_E$. Theoretically, the impulse voltage wave shape is composed by the superposition of two exponential functions.

As mentioned before, the charging capacitor C_S is charged via a high voltage dc supply through the rectifier. In the simulation, the initial condition for C_S is set to 8,600V and then it is discharged by closing switch S_1 (sparks in the sphere gap). Then, the simulation result is taken from the voltage across the load capacitor C_B . The simulation result in Figure 10 shows that, the peak impulse voltage is 8,600V with the front time t_f of 1.5 μ s and the tail time t_t of 47 μ s.

5.2 Additional switches

Figure 11 shows the circuit configuration that is almost similar with the previous circuit in Figure 9, except that there are two additional normally closed (NC) switches S_2 and S_3 . Later, in the hardware development, both switches are replaced by the IGBT switch.

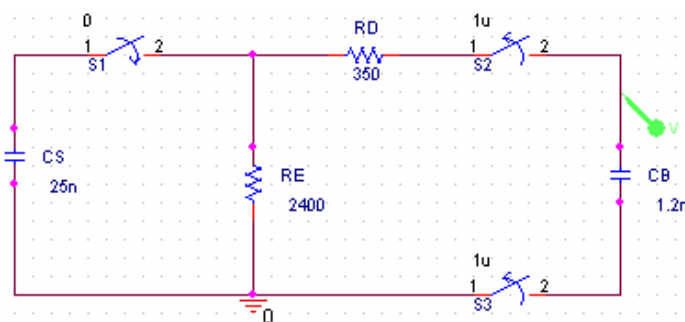


Fig. 11. Single impulse voltage generator circuit with additional two normally closed (NC) switches

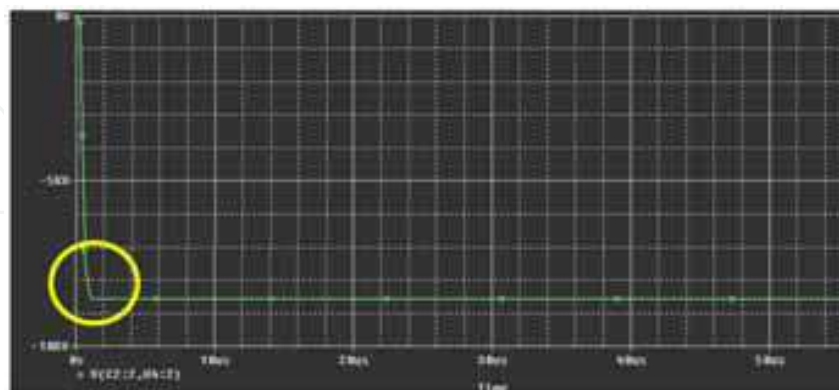


Fig. 12. Peak voltage 8.6kV is hold at $t \geq 1.5\mu$ s

The purpose of using these switches is to isolate C_B from any connection after the peak voltage has been attained in the capacitor. According to the Figure 2, the peak value of impulse voltage occurs at 1.5 μ s. Both NC (S_2 and S_3) switch are setting to be open at 1 μ s

where the setting time is less than the time where the peak impulse voltage occurred. It is because the switches that have been used in the simulation have a delay about $0.5\mu\text{s}$. For that reason, even though the switches are set at $1\mu\text{s}$, the simulation result had showed that the both switches are operated at approximately $1.5\mu\text{s}$.

Referring to the Figure 12, the voltage of the load capacitor C_B is not decaying after reach the peak value at $1.5\mu\text{s}$ (yellow circle). It proves that, when the both switches applied in the circuit, the voltage is slightly maintained. It shows that, the capacitor C_B is not able to discharge because it was isolated from any connection.

6. Laboratory experimental testing

In order to facilitate easy understanding, this subchapter will be divided into three stages. In Stage 1, the intention is to build up a 4.2kV single stroke impulse voltage. Therefore, the right combination of resistance value and capacitance value has to be clarified in order to get the standard impulse wave shape. The wave shape must follow the standard parameter, which is $1.2/50\mu\text{s}$ and when it is complete, now a mock lightning (source of lightning) in a small scale is ready and can be applied for the testing in Stage 2 and stage 3.

In Stage 2, the generated impulse voltage produced in Stage 1 is applied to a number of sample capacitors with different capacitance value. The important electrical parameter that need to gather is the voltage wave shape for each capacitor that has been tested. The wave shape will give an information about the sample capacitor characteristics such as the voltage capture, voltage store, voltage dissipated, the energy efficiency as well as charging and discharging time of the sample capacitor.

In Stage 3, high speed switching device is applied in the testing circuit. In the beginning, the sample capacitor will be charged by the impulse voltage. Then, it is isolated from any connection with the aid of high speed switching device. After approximately 15 minutes, the voltage waveform in the capacitor will be observed and this waveform is the data that required to be obtained.

6.1 Stage 1: impulse generation

As previously mentioned in section 5.1, the standard impulse lightning wave shapes is generated by using the single stage impulse voltage generator. The standard wave shapes has $1.2\mu\text{s}$ for the front time and $50\mu\text{s}$ for the tail time.



Fig. 13. Circuit arrangement for the testing in stage 1

The equipments that need to be used to setup the single impulse generator as shown in Figure 13 are consisted of Single Phase AC Voltage Test Transformer, HV rectifier, charging and load capacitor, wave shaping resistance, sphere gap, grounding rod, voltage divider, HV probe and oscilloscope.

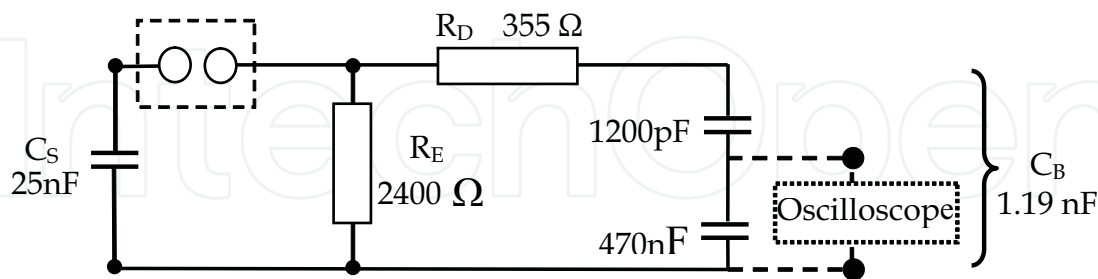


Fig. 14. Circuit diagram for stage 1 testing

By using the single stage impulse voltage generator circuit arrangement as shown in Figure 14, the desired impulse voltage wave shape has been achieved by choosing the correct resistance values for R_D and R_E as well as the capacitance values for C_S and C_B . In order to verify the impulse wave shape parameters, a digital oscilloscope is used to capture the experimental impulse voltage wave shapes with conjunction with the voltage divider. Besides that, the value of C_S , C_B , R_D and R_E are fixed in order to get a sustained 1.2/50 μ s wave shape. This is because the testing in the stage 2 and stage 3 will use the same magnitude of impulse voltage.

6.1.1 Front time, tail time and peak voltage of the experimental wave shape

Table 2 shows the right combination of the capacitance and resistance value for C_S , C_B , R_D and R_E that connected as shown in Figure 13 and Figure 14. In order to obtain the resistance and capacitance value, equation (1) and equation (2) in section 5.1 is used. As a result, the front time t_f and tail time t_t for the generated impulse voltage are 1.3 μ s and 45 μ s respectively. This value is slightly different from the standard impulse wave shape. However, it is accepted for the reason that the experimental value is still under the tolerance of impulse wave shape parameter, which is +8.3% for the t_f and -10% for the t_t .

Standard Impulse Voltage Waveshape 1.2/50 μ s	
Value of charging capacitance, C_S	25 nF
Value of load capacitance, C_B	1.19 nF
Value of resistance, R_D	355 Ω
Value of resistance, R_E	2400 Ω
Front Time, t_f simulation	1.51 μ s
Tail Time, t_t simulation	47.0 μ s
Front Time, t_f calculation	1.21 μ s
Tail Time, t_t calculation	44.0 μ s
Front Time, t_f experimental	1.30 μ s
Tail Time, t_t experimental	45.0 μ s

Table 2. Value of C_S , C_B , R_D and R_E that was used to obtain the standard impulse

Figure 15 and Figure 16 are the experimental impulse wave shapes that were recorded by using a digital oscilloscope. This is the output produced from the single stage impulse voltage generator. According to the experimental wave shape, the peak of the impulse voltage is 4,200V.

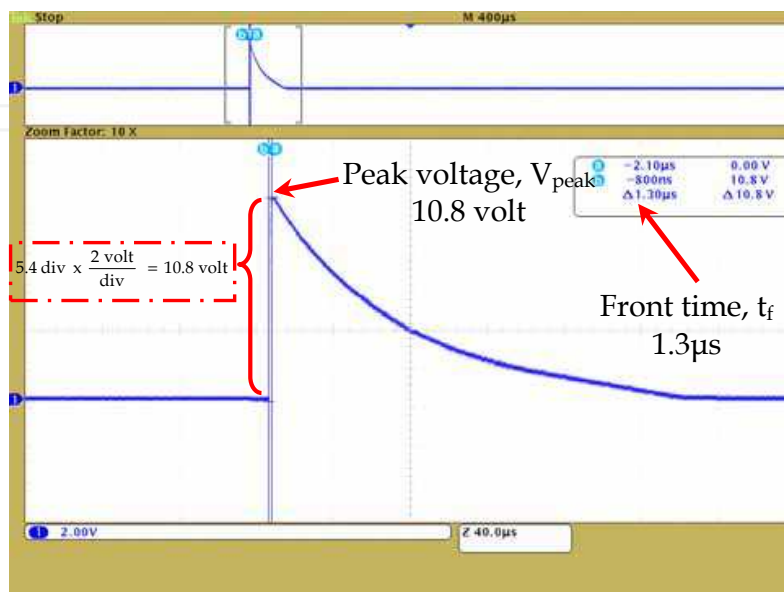


Fig. 15. Front time t_f of the experimental impulse voltage wave shape

In Figure 15, each division represents 2 volts and the peak voltage magnitude is 5.4 divisions. However, this is not the actual value of the peak voltage. To obtain the actual peak voltage, the reading is multiplied with the capacitive voltage divider ratio and finally recorded as an actual peak voltage. The capacitive voltage divider ratio is 392. As a result, the actual peak voltage is 10.8 volt x 392; equal to 4,200V.

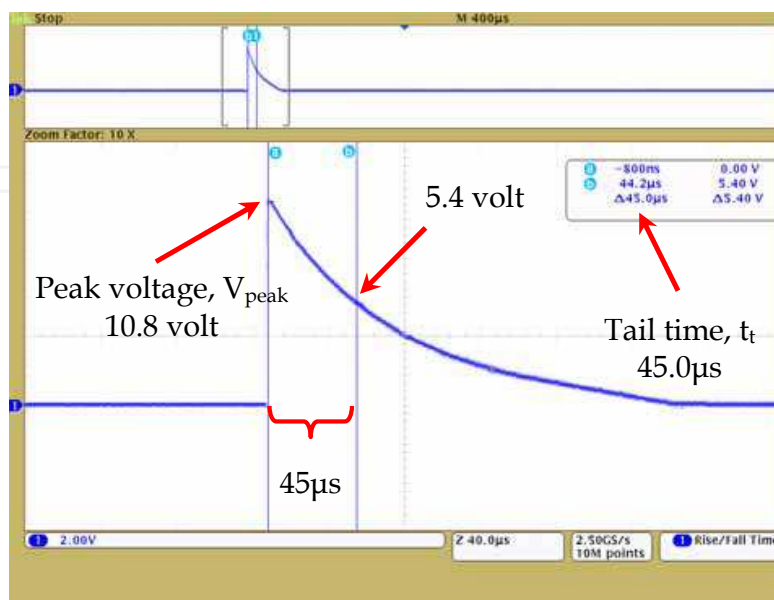


Fig. 16. Tail time t_t of the experimental impulse voltage wave shape

Meanwhile, Figure 16 illustrates the tail time, t_t of the experimental impulse voltage wave shape. It shows that the tail time, t_t is $45.0\mu\text{s}$ with the voltage at that time is half from the peak voltage of 10.8V , which is 5.4V . Finally, the lightning impulse voltage 4.2kV was generated. It is ready to be used in stage 2 and stage 3 for the laboratory experiment. This generated impulse voltage represents as a mock lightning in order to setup a small scale system for harvesting the lightning stroke.

6.2 Stage 2: energy collected in the capacitor

In this stage, it is intended to discover the electrical characteristics and the time response of the capacitor as energy storage element. In addition, the investigation is performed with varying the capacitance value and also increasing the number of sample capacitors. The characteristics of the sample capacitors have been described previously in section 3. If more than one unit sample capacitor is used in the experiment, the capacitors will be connected in parallel to acquire more capacitance.

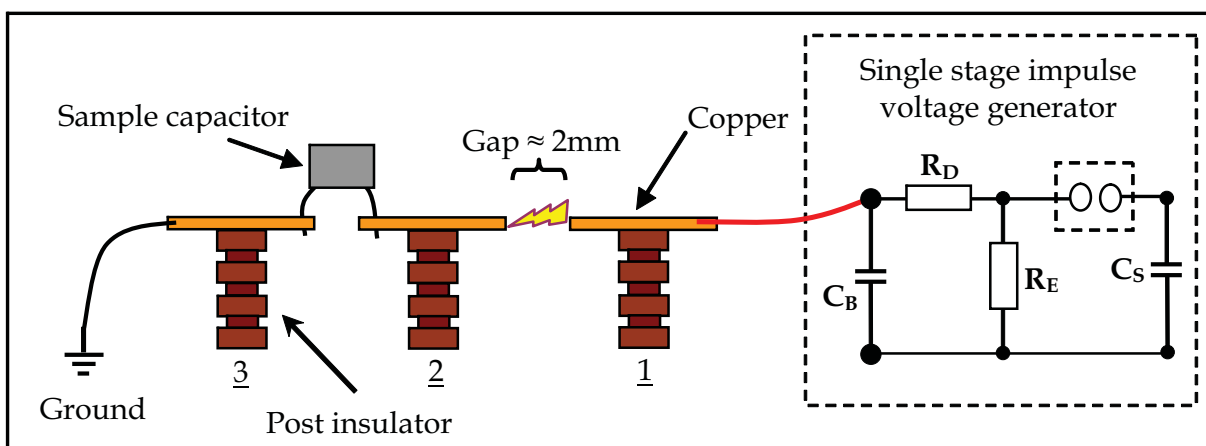


Fig. 17. Connection of sample capacitor with the impulse voltage generator.

In this stage, the process and the equipment involved in Stage 1 remain the same. Except, it has an additional circuit that is connected parallel with the load capacitor C_B . The additional circuit is consisted of three units of post insulator and sample capacitor.



Fig. 18. Flashover occurred between the gap (spark in the yellow circle)

As shown in Figure 17, post insulator no 1 is connected to the load capacitor C_B . Meanwhile, one unit of sample capacitor is connected between post insulator no 2 and no 3. The copper

bar at the post insulator no 1 and no 2 is not connected and it has a gap about 2mm. At the time when flashover occurs as shown in Figure 18, the gap will act as a closing switch and simultaneously completed the circuit and charging the sample capacitor. Throughout all these processes, the electrical characteristics and the time response of the sample capacitor can be obtained and measured via HV probe.

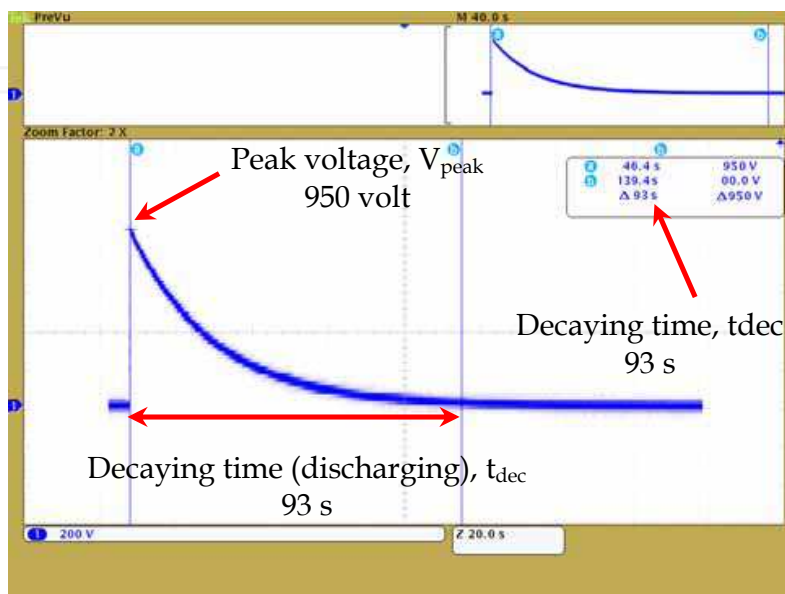


Fig. 19. Decaying time for one unit sample capacitor $0.22 \mu\text{F}$

The detailed information regarding the decaying period for one unit capacitor $0.22 \mu\text{F}$ (KNU1910) is illustrated in Figure 19. The decaying time from the peak voltage to the zero voltage is 93 seconds. After the data collection for the peak voltage, rising time and the decaying of one unit capacitor is completed, the process will be continued for two units as well as three units of capacitors connected in parallel.

In order to achieve a clearer picture regarding the voltage efficiency and dissipated voltage for all the sample capacitors used in the laboratory experiment, Figure 20, Figure 21 and Figure 22 can be used as references. In these figures, the pie charts illustrate the relationship between voltage and voltage efficiency for one unit, two units and three units of sample capacitor. It proves that the voltage efficiency has an inverse relation with the dissipated voltage, that is when the voltage efficiency increased, the voltage dissipated will be reduced and vice versa.

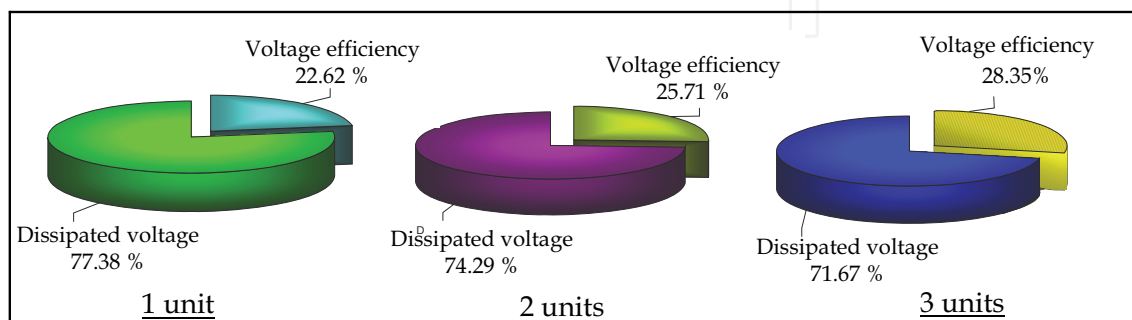


Fig. 20. Pie chart for sample capacitor $0.22 \mu\text{F}$ (KNU 1910)

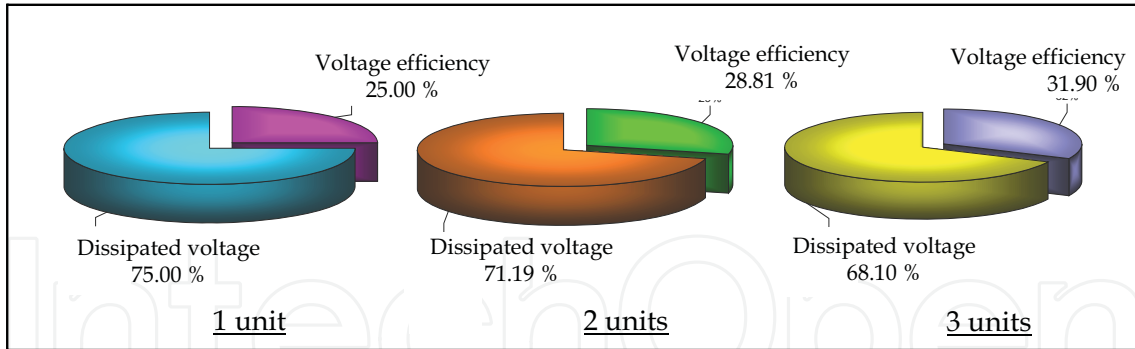


Fig. 21. Pie chart for sample capacitor 0.47µF (CBB20)

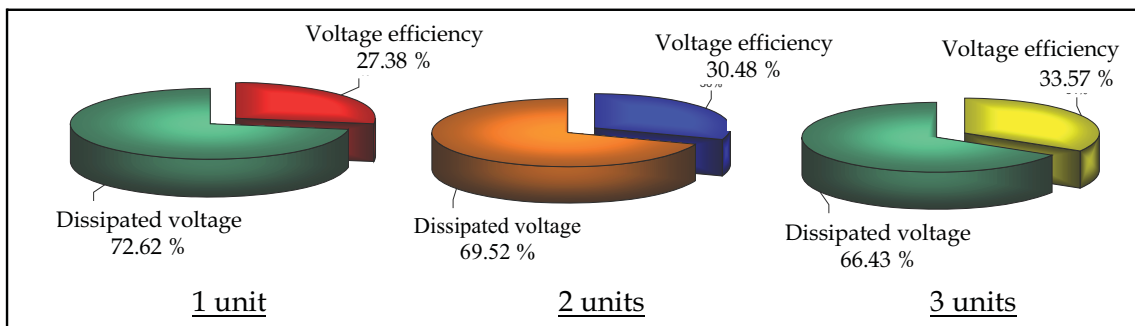


Fig. 22. Pie chart for sample capacitor 0.68µF (CBB20)

6.2.1 Experimental data analysis

In this section, the analysis is focused on the voltage stored V_{stored} , the charging and discharging time of the capacitor as well as the effect of capacitance value to the experimental result. Table 3 show the rough picture for the whole experimental result for stage 2.

Capacitor	0.22µF	0.47 µF	0.68 µF
Charging Voltage, V_s	←————→ Fix		
Peak Voltage, V_{peak}	□ □	□ □ □ □	□ □ □ □ □ □
Voltage Efficiency	□ □	□ □ □ □	□ □ □ □ □ □
Dissipated Voltage	□ □	□ □ □ □	□ □ □ □ □ □
Front Time, t_f	□ □	□ □ □ □	□ □ □ □ □ □
Decaying Time, t_{dec}	□ □	□ □ □ □	□ □ □ □ □ □

Table 3. Overall experimental data for stage 2

6.2.1.1 Analysis of experimental data for voltage stored V_{stored}

By referring to Figure 20, Figure 21 and Figure 22, the capacitors have the voltage efficiency approximately 22% to 33% and it has a dissipated voltage during the charging process. During the laboratory testing, the spark gap (gap between copper bar at post insulator no 1 and no 2) represents as a mock cloud. It is believed that the dissipated voltage was occurred at the spark gap and this situation is aligned with the theory of lightning energy. Most of the energy, dissipated in a sudden expansion that causes heating and ionization. The other fraction of energy will flow to the ground. According to that statement, that is the reason that the peak voltage V_{peak} in the sample capacitor is lower than the charging voltage V_s . Besides that, all the capacitors used in the experiment have the capability to capture the incoming impulse voltage. Seemingly, if more sample capacitors are used in the testing, more incoming energy can be attained. However, from the theory and the experimental result, it is confirmed that the biggest energy that could be harvested cannot be equal to the source of lightning energy. And the fact warns that, these efforts still need a reliability energy storage with a very high standard safety system as well as a very strong structure even though the energy can be tapped was not 100% from the source.

6.2.1.2 Analysis of experimental data for time response and capacitance value

In term of time response, the increment of capacitance value has given an effect to the decaying time or discharging time of the sample capacitor. The decaying time is increased in proportion with the increment of the capacitance value. The condition where the capacitor is slowly decaying can be manipulated in order to give a good prospect for future works such as to charge batteries or other electrical appliances.

In the testing, if more than one unit sample capacitor is used, the sample capacitors will be connected in parallel. The purpose is to increase the capacitance value in order to store more charge and voltage. This is the basic approach in determining the raise size of the plate area. The greater the plate area, the greater value of capacitance will be obtained. It is because, the larger plates area will result in more field flux (charge collected on the plates) and at the same time more field force (voltage across the plates) appears. According to the testing result, it was proved that, when greater capacitance value is obtained, the peak voltage V_{peak} , the stored voltage and energy efficiency also will be greater and increased.

6.3 Stage 3: high speed switching and energy stored

Basically, the experiment conducted in Stage 3 is almost similar with the Stage 2. The different is only the additional of high speed switching circuit using IGBT device. The purpose of the IGBT switch is to isolate the capacitor from any connection. In the beginning, the IGBT switch is set to be in a close position. Then, the impulse voltage is applied to charge the sample capacitor. Then, the switch will be opened and simultaneously disconnect the capacitor from any connection in order to fetter the capacitor from discharging.

Before the switching circuit is on, the condition of the IGBT switch is normally open. When the circuit is on, the IGBT switch from normally open will be in close position. According to the program instructions, the PIC controller will start to count until a few microsecond. Then, the IGBT switch from close position will be opened and at the same time, the capacitor is disconnected from any connection. The capacitor is left for about 900 seconds (isolating time) before reconnect to the ground connection. Finally, the voltage across the capacitor as energy storage element is measured once again in order to investigate the remaining voltage. Figure 23 illustrate the location of IGBT switch in the testing circuit.

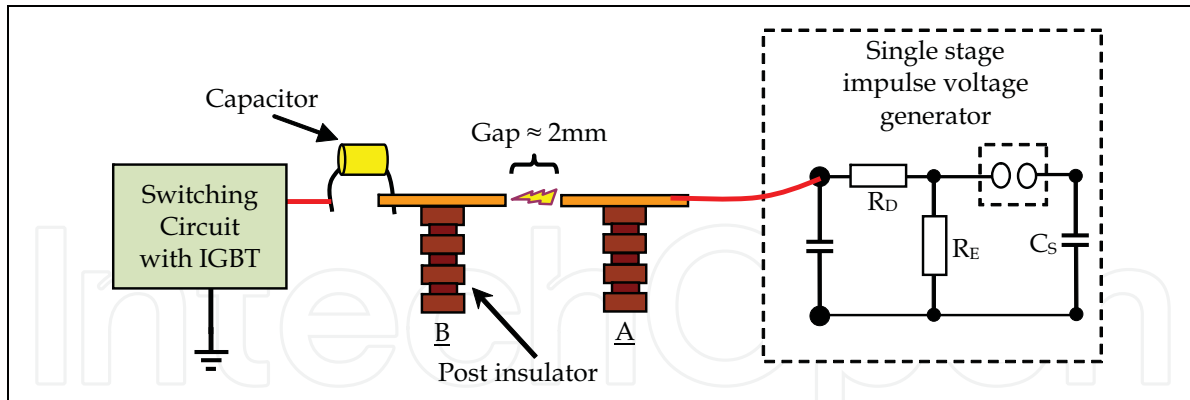


Fig. 23. IGBT switch is placed in series with the sample capacitors

6.3.1 Testing result: characteristics of the sample capacitor

Figure 24 and Figure 25 show the voltage waveform against the time across one unit of sample capacitor 0.22 μ F (KNU1910). These figures show the step by step explanation concerning the voltage behavior in the sample capacitor. Later, it can be seen that, different types of sample capacitors will give a dissimilar result in terms of the stored voltage, voltage losses and also the time response.

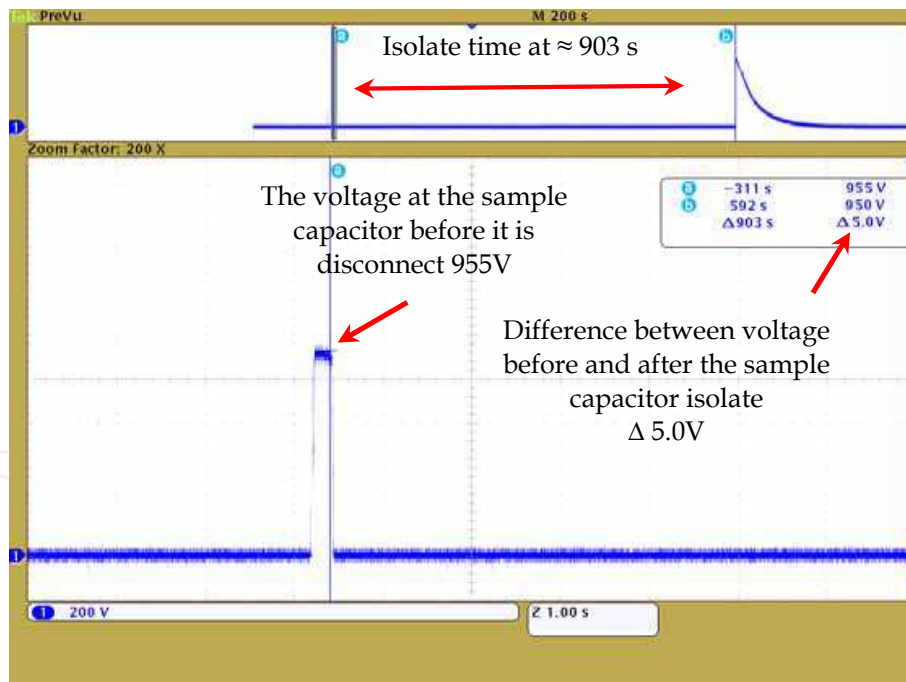


Fig. 24. The capacitor 0.22 μ F is isolated for 903 second after the switch opens

In Figure 24, the peak voltage in the sample capacitor is 955V. After 300 milliseconds, the switch opens and isolates the capacitor from any connections for approximately 900 seconds. Subsequently, after the isolating period (903 s \approx 15 min), the voltage in the sample capacitor 0.22 μ F (KNU1910) is 950V. The difference between the voltages before and after the capacitor was isolated is very small, which is only 5V.

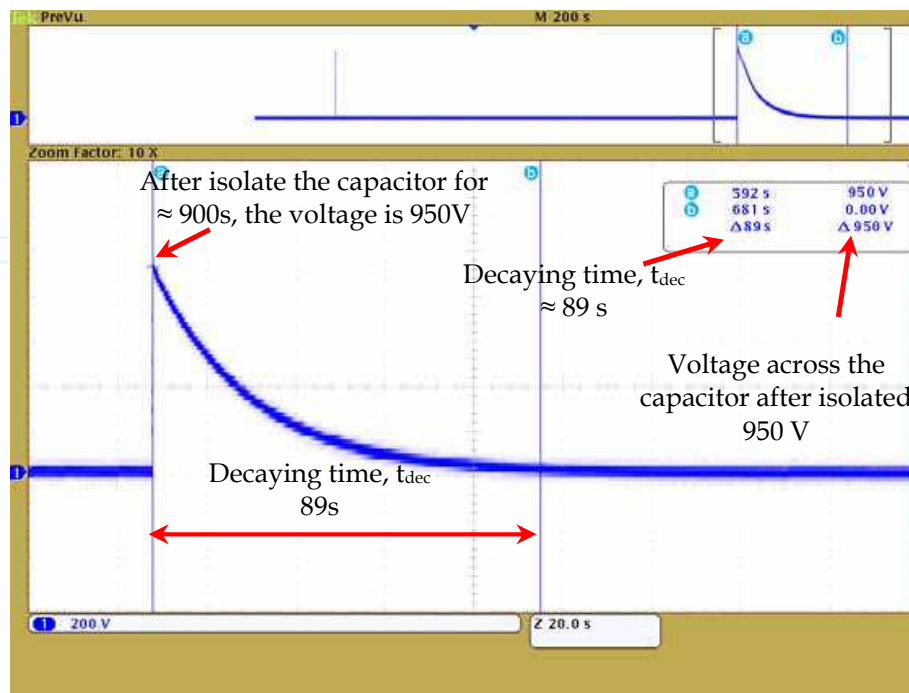


Fig. 25. Voltage waveform of the sample capacitor after isolating period.

Moreover, Figure 25 shows the voltage waveform after the isolating period where the sample capacitor 0.22 μ F (KNU1910) was reconnected with the ground connection. This figure illustrates that the decaying time is 87 second. The difference in terms of decaying time between stage 2 and stage 3 does not have much difference, where the discharging time for the stage 2 is 91 second and for stage 3 is 87 second.

However, the performance of the capacitor 0.46 μ F (CBB20) and 0.68 μ F (CBB20) was not as good as the capacitor 0.22 μ F (KNU1910). Both capacitors have no capability to retain and sustain the voltage during the isolating period. Besides that, there was a huge difference between the decaying time for stage 2 and stage 3.

6.3.2 Experimental data analysis

Table 4, Table 5 and Table 6 shows the step by step calculation in determining the energy stored and the energy efficiency of the sample capacitor. Thus, determining the decaying voltage function $v(t)$ for every sample capacitor will be the basic step for the energy calculations. Once, the decaying voltage function $v(t)$ is obtained, it will be used to calculate the average voltage V_{ave} , the energy stored E_{stored} and the energy efficiency $E_{efficiency}$ of the sample capacitor.

Throughout the testing in stage 3, the source voltage V_{source} is fixed at 4.2kV. It means that, the energy supplied by the impulse voltage generator to the sample capacitor is maintained. Herewith is the calculation for the energy supplied from the impulse voltage generator.

$$\text{Energy source, } E_S = 0.5 C_s V_s^2 = 0.5 (2500 \text{ pF}) (4200\text{V})^2 = 0.2205 \text{ Joule}$$

	0.22 μF (KNU1910)		
No of capacitor use	1 unit	2 unit	3 unit
Time constant, τ	31 second	59 second	92 second
Voltage Decay, $v(t)$	$950 e^{-\frac{t}{31}}$	$1070 e^{-\frac{t}{59}}$	$1180 e^{-\frac{t}{92}}$
Average Voltage, V_{ave}	$\frac{1}{93} \int_0^{93} 950 e^{-\frac{t}{31}} dt$ = 300.92 V	$\frac{1}{184} \int_0^{184} 1070 e^{-\frac{t}{59}} dt$ = 327.93 V	$\frac{1}{271} \int_0^{271} 1180 e^{-\frac{t}{92}} dt$ = 379.53 V
Energy Stored, E_{stored}	$\frac{1}{2} (0.22 \mu\text{F}) (300.92\text{V})^2$ = 9.96×10^{-3} J	$\frac{1}{2} (0.44 \mu\text{F}) (327.93\text{V})^2$ = 23.66×10^{-3} J	$\frac{1}{2} (0.66 \mu\text{F}) (379.53\text{V})^2$ = 47.53×10^{-3} J
Energy Efficiency $= \frac{E_{\text{stored}}}{E_{\text{source}}} \times 100\%$	$= \frac{9.96 \times 10^{-3} \text{ J}}{220.50 \times 10^{-3} \text{ J}} \times 100\%$ = 4.52 %	$= \frac{23.66 \times 10^{-3} \text{ J}}{220.50 \times 10^{-3} \text{ J}} \times 100\%$ = 10.73 %	$= \frac{47.53 \times 10^{-3} \text{ J}}{220.50 \times 10^{-3} \text{ J}} \times 100\%$ = 21.55 %

Table 4. Energy efficiency and the energy stored of the capacitor 0.22 μF

	0.47 μF (CBB20)		
No of capacitor use	1 unit	2 unit	3 unit
Time constant, τ	47 second	90 second	126 second
Voltage Decay, $v(t)$	$1050 e^{-\frac{t}{90}}$	$1210 e^{-\frac{t}{90}}$	$1340 e^{-\frac{t}{126}}$
Average Voltage, V_{ave}	$\frac{1}{140} \int_0^{140} 1050 e^{-\frac{t}{47}} dt$ = 334.57 V	$\frac{1}{268} \int_0^{268} 1210 e^{-\frac{t}{90}} dt$ = 371.07 V	$\frac{1}{396} \int_0^{396} 1340 e^{-\frac{t}{126}} dt$ = 407.96 V
Energy Stored, E_{stored}	$\frac{1}{2} (0.47 \mu\text{F}) (334.57\text{V})^2$ = 26.31×10^{-3} J	$\frac{1}{2} (0.94 \mu\text{F}) (371.07\text{V})^2$ = 64.72×10^{-3} J	$\frac{1}{2} (1.41 \mu\text{F}) (407.96\text{V})^2$ = 117.33×10^{-3} J
Energy Efficiency $= \frac{E_{\text{stored}}}{E_{\text{source}}} \times 100\%$	$= \frac{26.31 \times 10^{-3} \text{ J}}{220.50 \times 10^{-3} \text{ J}} \times 100\%$ = 11.93 %	$= \frac{64.72 \times 10^{-3} \text{ J}}{220.50 \times 10^{-3} \text{ J}} \times 100\%$ = 29.53 %	$= \frac{117.33 \times 10^{-3} \text{ J}}{220.50 \times 10^{-3} \text{ J}} \times 100\%$ = 53.21 %

Table 5. Energy efficiency and the energy stored of the capacitor 0.47 μF

No of capacitor use	0.68 μ F (CBB20)		
	1 unit	2 unit	3 unit
Time constant , τ	68 second	121 second	171 second
Voltage Decay, $v(t)$	$1150 e^{-\frac{t}{68}}$	$1280 e^{-\frac{t}{121}}$	$1410 e^{-\frac{t}{171}}$
Average Voltage, V_{ave}	$\frac{1}{205} \int_0^{205} 1150 e^{-\frac{t}{68}} dt$ = 362.75 V	$\frac{1}{385} \int_0^{385} 1280 e^{-\frac{t}{121}} dt$ = 385.59 V	$\frac{1}{556} \int_0^{556} 1410 e^{-\frac{t}{171}} dt$ = 410.45 V
Energy Stored, E_{stored}	$\frac{1}{2} (0.68 \mu F) (362.75V)^2$ = 44.74×10^{-3} J	$\frac{1}{2} (1.36 \mu F) (385.59V)^2$ = 101.10×10^{-3} J	$\frac{1}{2} (2.04 \mu F) (410.45V)^2$ = 171.83×10^{-3} J
Energy Efficiency = $\frac{E_{stored}}{E_{source}} \times 100\%$	$= \frac{44.74 \times 10^{-3} J}{220.50 \times 10^{-3} J} \times 100\%$ = 20.29 %	$= \frac{101.10 \times 10^{-3} J}{220.50 \times 10^{-3} J} \times 100\%$ = 45.85 %	$= \frac{171.83 \times 10^{-3} J}{220.50 \times 10^{-3} J} \times 100\%$ = 77.93 %

Table 6. Energy efficiency and the energy stored of the capacitor 0.68 μ F

6.3.3 Analysis of experimental data for voltage stored and energy efficiency

As mentioned before, the energy supplied by the lightning impulse voltage generator is maintained at approximately 0.2205 Joule. According to Table 4, Table 5 and Table 6, the measurement data shows that the capacitors used in the testing have the energy efficiency in the range of 4.52% to 77.93%. The data also proved that the energy efficiency increases together with the increment of capacitance value.

Instead of the capacitance value, there are a few factors that will give a significance effect to the voltage stored as well as the energy efficiency. One of the factors is the type of capacitor that was used in the experiments. It knows that, the energy efficiency is proportional with the stored voltage. From the measurement result, only the capacitor 0.22 μ F (KNU1910) is capable of sustaining the voltage compared to other sample capacitors. In other words, even though the energy efficiency for this capacitor is lower from other sample capacitor, only a small voltage losses occurred. The opposite of that, the sample capacitors 0.47 μ F (CBB20) and 0.68 μ F (CBB20) suffer a huge voltage losses during the isolating period. It means that, there will be sometime when the voltage stored in both these capacitor reduces to the zero voltage and causes a zero energy efficiency.

Another factor that is responsible in obtaining the higher energy efficiency is the tapping method. It is because, the tapping system will be the primary role to attract and capture the lightning energy. It means that, this part have to captured as much as the energy supplied and also transfer the energy to the storage devices.

The last factor is the effectiveness of the high speed switching device. The main task of this switching device is to facilitate the capacitors to sustain the charge and the voltage during the separating period. By referring to the measurement data, the high speed switching applied in the testing circuit gave a good performance.

7. Discussion and conclusion

The present work has been directed towards a better understanding of harvesting the lightning energy in a small scale system. In order to achieve the above , the work was

focused on the development of a small scale laboratory experiment. It was done by injecting the capacitor, which represents an energy storage element, with lightning impulse voltage as a mock lightning. Prior to this, a computer simulation using Pspice was done in order to develop a reliable testing circuit in the laboratory.

The simulation work provides an understanding on how to generate the single stroke impulse voltage. Besides that, it also verifies that the circuit that uses fast switching is capable of retaining the incoming lightning impulse voltage. In addition, the simulation circuit was considered as a reference for the circuit arrangement in the lab.

In the experimental work, it should be noted that the direct tapping approach is suitable for the small scale system. This approach is capable of attracting about a quarter of the incoming lightning impulse voltage and simultaneously charging the sample capacitor. Besides that, the employment of the high speed switching in the testing circuit for the isolation purpose also gives a meaningful outcome. The switching circuit is able to separate the storage device from the circuit connection. However, it has voltage losses that occurred in a few of the sample capacitors during the isolating period. This happened not because of the switch, but due to the losses that came from the sample capacitor itself.

The effects of single stroke impulse voltage 1.2/50 μ s, 4.2kV on the electrical characteristics of the sample capacitor have been determined from the experimental work. There were significant effects on the electrical characteristics such as peak voltage, stored voltage, charging time, discharging time as well as the energy efficiency of the sample capacitor for a single stroke impulse voltage.

Clearly, the stored voltage and the energy efficiency of the sample capacitor is extremely increased in proportion with the increment of the capacitance value. By referring to the result and the analysis that have been achieved, the capacitor 0.22 μ F(KNU1910) has the capability to store energy compared to the other samples which are the 0.47 μ F(CBB20) capacitor, and the 0.68 μ F(CBB20) capacitor.

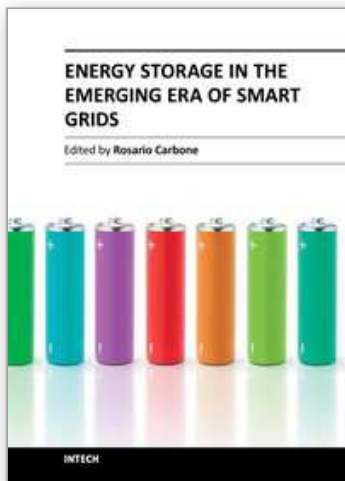
Moreover, the experimental results also confirmed that the small scale system constructed which consists of the tapping system and the high speed switching are successfully implemented. It gives significant effects on the electrical characteristics of the sample capacitor subjected to a single stroke impulse voltage of 1.2/50 μ s, 4.2kV. In particular, the electrical characteristics such as the voltage stored, the response time and the energy efficiency of the sample capacitor is proportional to the value of capacitance and the type of capacitor that have been used.

It proves that, the outcome can be improved as long as the energy storage devices, the fast switching circuit and the tapping system are correctly chosen. Generally, the way of testing that was conducted in this project may not be accurate enough to represent the model system for harvesting the lightning energy. However, from the results obtained, it is found to be acceptable.

The race to develop the technology in harvesting the lightning energy among the scientist and engineers is ongoing. Since, there are no mature studies of this technology and the scientific literature is not easily found, therefore this project is carried out to be as a sensible part of the research studies. In addition, the experimental result gives a meaningful indicator regarding the effort to create a small scale system for harvesting the lightning impulse energy. It should be noted that the final system of this project would provide an understanding of the system principle and furthermore give a significant contribution for further research. Finally, it is hoped that this project will be able to contribute towards making the process of harvesting lightning energy a reality.

8. References

- Abidin, H.Z. & Ibrahim, R. (2003). Thunderstorm Day and Ground Flash Density In Malaysia. *Proceedings of National Power and Energy Conference, (PECon 2003)*, pp. 217-219, ISBN 0-7803-8208-0, Bangi, Kuala Lumpur, Malaysia, December 15-16, 2003
- Karthick S. & Jason G., (2006). Lightning as Atmospheric Electricity. *Canadian Conference on Electrical and Computer Engineering, (CCECE '06)*, pp. 2258-2261, ISBN 1-4244-0038-4, Ottawa, Canada, May 7-10, 2006
- Rebeiro, P.F.; Johnson, B.K.; Crow, M.L.; Arsov, A. & Liu, Y.; (2001). Energy Storage System for Advanced Power Application, *Proceedings of the IEEE*, Vol.89, Issue.12, (December 2001), pp. 1744-1756, ISSN 0018-9219
- Uman, M.A. (1994). Natural Lightning. *IEEE Transactions on Industry Applications*, Vol.30, Issue.3, (June 1994), pp. 785-790, ISSN 0093-9994
- Yao, Y.Y.; Zhang, D.L. & Xu, D.G. (2006). A Study of Supercapacitor Parameters and Characteristics. *International Conference on Power System Technology, (PowerCon 2006)*, pp. 1-4, ISBN 1-4244-0110-0, Chongqing, China, October 22-26, 2006
- Kumar, B. (1992). Magnetic Energy Storage Devices for Small Scale Applications. *IEEE Aerospace and Electronic Systems Magazine*, Vol.7, Issue.11, (November 1992), pp. 12-17, ISSN 0885-8985
- Chowdhuri, P. (2001). Parameter of Lightning Stroke and Their Effect on Power System. *IEEE/PES Transmission and Distribution Conference and Exposition*, pp. 1047-1051, ISBN 0-7803-7285-9, Atlanta, USA, October 28-November 02, 2001
- Hefner, A.R. Jr. & Diebolt, D.M. (1994). An Experimentally Verified IGBT Model Implemented in the Saber Circuit Simulator. *IEEE Transactions on Power Electronics*, Vol.9, Issue.5, (September 1994), pp. 532-542, ISSN 0085-8993
- Microchip Technology Inc. (2001). PIC16F84A Data Sheet, Available from <http://ww1.microchip.com/downloads/en/devicedoc/35007b.pdf>
- Ibrahim, D. (2008). Advanced PIC Microcontroller Projects in C: From USB to RTOS with the PIC18F Series, In: C Programming Language, 119-165, ISBN 978-0-7506-811-2, Oxford UK, Newnes
- Yao, Y. Y.; Zhang, D. L. & Xu, D. G. (2006) A Study of Supercapacitor Parameters and Characteristics. *Power System Technology, 2006. PowerCon 2006. International Conference on*. pp. 1-4, ISBN 1424401100, Chongqing, China, October 22-26, 2006.
- Wei, L. & JOOS, G. (2008) A Power Electronic Interface for a Battery Supercapacitor Hybrid Energy Storage System for Wind Applications. *Power Electronics Specialists Conference, 2008. PESC 2008. IEEE*, pp. 1762-1768, ISBN 978-1-4244-1667-7, Rhodes, Greece, June 15-19, 2008.
- Pagano, M. & Piegari, L. (2004) Supercapacitor Flywheel for High Power Electrochemical Sources. *Power Electronics Specialists Conference, 2004. PESC 04. 2004 IEEE 35th Annual*. pp. 718-723 (Vol.1), ISBN 0-7803-8399-0, June 20-25, 2004..
- Swett, D. W. & Blanche, J. G. IV. (2005) Flywheel Charging Module for Energy Storage Used in Electromagnetic Aircraft Launch System. *12th Symposium on Electromagnetic Launch technology, IEEE Transactions on*, Vol.41, pp. 525-528, ISBN 0-7803-8290-0, Snowbird, Utah, May 25-28, 2005.



Energy Storage in the Emerging Era of Smart Grids

Edited by Prof. Rosario Carbone

ISBN 978-953-307-269-2

Hard cover, 478 pages

Publisher InTech

Published online 22, September, 2011

Published in print edition September, 2011

Reliable, high-efficient and cost-effective energy storage systems can undoubtedly play a crucial role for a large-scale integration on power systems of the emerging “distributed generation” (DG) and for enabling the starting and the consolidation of the new era of so called smart-grids. A non exhaustive list of benefits of the energy storage properly located on modern power systems with DG could be as follows: it can increase voltage control, frequency control and stability of power systems, it can reduce outages, it can allow the reduction of spinning reserves to meet peak power demands, it can reduce congestion on the transmission and distributions grids, it can release the stored energy when energy is most needed and expensive, it can improve power quality or service reliability for customers with high value processes or critical operations and so on. The main goal of the book is to give a date overview on: (I) basic and well proven energy storage systems, (II) recent advances on technologies for improving the effectiveness of energy storage devices, (III) practical applications of energy storage, in the emerging era of smart grids.

How to reference

In order to correctly reference this scholarly work, feel free to copy and paste the following:

Mohd Farriz Basar, Musa Yusop Lada and Norhaslinda Hasim (2011). Lightning Energy: A Lab Scale System, Energy Storage in the Emerging Era of Smart Grids, Prof. Rosario Carbone (Ed.), ISBN: 978-953-307-269-2, InTech, Available from: <http://www.intechopen.com/books/energy-storage-in-the-emerging-era-of-smart-grids/lightning-energy-a-lab-scale-system>

INTECH
open science | open minds

InTech Europe

University Campus STeP Ri
Slavka Krautzeka 83/A
51000 Rijeka, Croatia
Phone: +385 (51) 770 447
Fax: +385 (51) 686 166
www.intechopen.com

InTech China

Unit 405, Office Block, Hotel Equatorial Shanghai
No.65, Yan An Road (West), Shanghai, 200040, China
中国上海市延安西路65号上海国际贵都大饭店办公楼405单元
Phone: +86-21-62489820
Fax: +86-21-62489821

© 2011 The Author(s). Licensee IntechOpen. This chapter is distributed under the terms of the [Creative Commons Attribution-NonCommercial-ShareAlike-3.0 License](https://creativecommons.org/licenses/by-nc-sa/3.0/), which permits use, distribution and reproduction for non-commercial purposes, provided the original is properly cited and derivative works building on this content are distributed under the same license.

IntechOpen

IntechOpen